博 士 学 位 論 文

1.5-T MRI を 用 い た BB Cube イ メ ー ジ と
3D-SPGR イメージでの脳腫瘍の病巣増強の比較

近 畿 大 学 大 学 院 医 学 研 究 科
医学系放射線診断・画像応用治療学

長 谷 川 　 博 　 一

同　意　書

平成29年 6月 2日

近畿大学大学院
医学研究科長　殿

共著者 ＿＿若山哲也＿＿ ㊞　　　共著者 ＿＿三好光晴＿＿ ㊞

共著者 ＿足利竜一朗＿ ㊞　　　共著者 ＿＿岡嶋　馨＿＿ ㊞

共著者 ＿西村恭昌＿＿ ㊞　　　共著者 ＿村上卓道＿＿ ㊞

共著者 ＿＿＿＿＿＿＿ ㊞　　　共著者 ＿＿＿＿＿＿＿ ㊞

共著者 ＿＿＿＿＿＿＿ ㊞　　　共著者 ＿＿＿＿＿＿＿ ㊞

論文題目

Comparison of lesion enhancement between BB Cube and 3D-SPGR images
for brain tumors with 1.5-T magnetic resonance imaging

下記の学位論文提出者が、標記論文を貴学医学博士の学位論文（主論文）
として使用することに同意いたします。
また、標記論文を再び学位論文として使用しないことを誓約いたします。

記

1. 学位論文提出者氏名　　　　長谷川　博一

2. 専攻分野　　　　　　　　　医学系　放射線診断・画像応用治療 学

近畿大学大学院医学研究科

Doctoral   Dissertation

Comparison of lesion enhancement between BB Cube and 3D-SPGR images for brain tumors with 1.5-T magnetic resonance imaging

Hirokazu Hasegawa

Department of Radiology, Image-Applied Therapy, Major in Medical Sciences

Kindai University Graduate School of Medical Sciences

(Director : Prof. Takamichi Murakami)

August 2017

Comparison of lesion enhancement between BB Cube and
3D-SPGR images for brain tumors with 1.5-T magnetic resonance imaging

Hirokazu Hasegawa [1], Ryuichiro Ashikaga [1], Kaoru Okajima [1], Tetsuya Wakayama [2], Mitsuharu Miyoshi [2], Yasumasa Nishimura [3], Takamichi Murakami [4]

[1] Department of Radiology, Nara Hospital, Kindai University Faculty of Medicine
[2] GE Healthcare Japan, MR Applications and Workflow, Asia Pacific
[3] Department of Radiation Oncology, Kindai University Faculty of Medicine
[4] Department of Radiology, Kindai University Faculty of Medicine
(Director：Prof. Takamichi Murakami)

Abstract

Purpose：This study aimed to compare the detectability of neoplastic lesion enhancement after gadolinium-based contrast media injection in three-dimensional T1-weighted black blood CUBE（3D-T1W BB CUBE）and three-dimensional T1-weighted fast spoiled gradient-echo（3D-T1W fast SPGR）images obtained with 1.5-T magnetic resonance imaging（MRI）.

Materials and Methods：Phantom and clinical studies were performed to compare lesion detectability and contrast ratio（CR）between 3D-T1W BB CUBE and 3D-T1W fast SPGR pulse sequences.

Results：In the phantom study, the CRs for 3D-T1W BB CUBE and 3D-T1W fast SPGR were equivalent at low gadolinium concentrations （0.125-1.25 mmol/L）. In the clinical study, the detectability in the two modalities was similar for enhanced lesions ≥ 5 mm, but was significantly better in 3D-T1W BB CUBE for lesions < 5 mm（p=0.011）. Similarly, the CRs in both modalities were similar for lesions ≥ 5 mm（0.66±0.36 vs. 0.56±0.30, p=0.153）, but significantly lower in 3D-T1W BB CUBE images for lesions < 5 mm（0.29±0.19 vs. 0.39±0.21, p=0.006）.

Conclusions：Contrast 3D-T1W BB CUBE imaging appear more sensitive than 3D-T1W fast SPGR imaging for detecting neoplastic lesion enhancement in the clinical setting using a 1.5-T MRI scanner, particularly for lesions < 5 mm in diameter.

Key words：CUBE, Spoiled gradient-echo（SPGR）, Black blood（BB）imaging, Contrast enhancement, Magnetic resonance imaging

Introduction

Metastases to the brain are common in patients with systemic cancer, resulting in the alteration of disease prognosis and treatment. Optimum therapeutic strategies for brain metastasis are determined on the basis of the number, size, and location of the brain metastases, identified using contrast-enhanced magnetic resonance imaging (MRI). Accurate detection of small brain metastases is therefore critical. Recent advances in MRI machine hardware and software have led to new capabilities in scanning, primarily directed at improving spatial resolution, scanning speed, and surface absorption ratio (SAR).

Two-dimensional (2D) contrast-enhanced MRI using T1-weighted spin-echo (SE) or 3-dimensional (3D) gradient-echo sequences are most commonly used for detecting and evaluating intracranial lesions [1−3]. Recent studies have reported better visualization of small tumors in thin 3D gradient-echo sequences such as 3D T1-weighted fast spoiled gradient-echo (3D-T1W fast SPGR) than in conventional 2D T1-weighted SE images [1, 4]. It has also been reported that 3D fast-spin-echo (FSE) sequences such as CUBE (GE Healthcare), SPACE (Sampling Perfection with Application-optimized Contrasts using different flip angle Evolution; Siemens Healthcare), and VISTA (Volume ISotropic Turbo spin echo Acquisition, Philips) allow better detection of brain metastases compared to 3D fast gradient sequences [3−5].

CUBE is a 3D FSE sequence that can be employed with T1-weighted (T1W), T2-weighted (T2W), and proton density-weighted imaging to obtain high spatial resolution volume data [2]. By applying a modulated flip angle train to refocus radio-frequency pulses, CUBE produces clearer images with 3-T MRI, even if the echo train length is more than 100, and reduces the SAR. Various preparation techniques, such as spatial presaturation, double inversion recovery, and motion-sensitizi z ng magnetization preparation, can be applied for black blood (BB) imaging [1]. By applying a BB preparation technique to a 3D FSE sequence, thin-slice whole-brain T1W BB CUBE images can be obtained without flow-related artifacts. SungWoon et al. reported that suppression of arterial flow as well as cortical veins was useful when screening for small lesions and could be considered a major advantage of this technique [2]. The above referenced studies used 3-T MRI to improve contrast enhancement, contrast-to-noise ratio (CNR), and resolution in an attempt to improve the detectability of small brain metastases [3−5]. However, the use of 3-T MRI is associated with a 4-fold higher SAR and a poorer white matter/gray matter contrast. Therefore, it is important to develop and study imaging sequence techniques that can achieve high contrast-enhancement and improve the detectability of small intracranial lesions through 1.5-T MR imaging.

The purpose of this study was to investigate the effect of contrast enhancement on the detectability of intracranial neoplastic lesions in 3D-T1W BB CUBE and 3D-T1W fast SPGR images obtained with a 1.5-T scanner. We first performed a phantom study to investigate contrast enhancement using varying concentrations of gadolinium-based contrast media with various spin and pulse sequences in a 1.5-T scanner. After confirming the feasibility of this approach, we compared contrast enhancement and lesion detectability in the 3D-T1W BB CUBE and 3D-T1W SPGR sequences of patients with intracranial neoplastic lesions.

Materials and Methods

MR imaging

MR imaging was performed using a 1.5-T scanner (GE Healthcare, Signa HDxt, WI) with a 12-channel phased-array head coil. 2D-T1W SE, 3D-T1W BB CUBE, and 3D-T1W fast SPGR pulse sequences were obtained in both the phantom/volunteer and clinical studies.

Phantom study

The purpose of the phantom study was to investigate the contrast properties of 2D-T1W SE, 3D-T1W BB CUBE, and 3D-T1W fast SPGR pulse sequences at varying concentrations of gadolinium-based contrast media (Magnevist; Bayer Schering Pharma, Berlin, Germany). The acquisition parameters for these sequences are shown in Table 1. Gadolinium dilutions were prepared in saline to concentrations of 0.125, 0.25, 0.5, 1.25, 2.5, and 5 mmol/L, corresponding to T1 values of 45 to 1100 ms. The phantom had dimensions of 37 mm × 25 mm × 59 mm and was placed near the volunteer's head. With each of the pulse sequences, the signal intensity (SI) of the phantom tube and that of the normal white matter (WM) of the volunteer were measured, and the contrast ratio (CR) was calculated using the following equation [5] :

CR = (SI of phantom – SI of normal WM) / SI of normal WM

The phantom study was conducted using a single volunteer and a single phantom. CR was measured only once per gadolinium concentration. As the purpose of the phantom study was primarily to investigate the feasibility of the study question, no statistical analyses were performed.

Clinical study

This study was approved by our institutional review board. From April to August 2013, 42 patients with suspicion of brain lesion were enrolled (19 men and 23 women; mean age: 59.4 years; range: 31–84 years). A subset of these patients had received prior radiotherapy for brain metastases. The investigators explained the study in detail and written informed consent was obtained from all subjects.

The clinical study was performed to compare lesion detectability and the contrast ratio between 3D-T1W BB CUBE and 3D-T1W fast SPGR pulse sequences. Post-contrast axial 3D-T1W BB CUBE and 3D-T1W fast SPGR pulse sequences were added to the routine MRI protocol, which consisted of pre-contrast axial T1W, T2W, and FLAIR and 1 min post-contrast coronal and axial 2D-T1W SE images. The dose of gadolinium was 0.1 mmol/kg. Acquisition parameters for the post-contrast scans are shown in Table 1. All scans were performed consecutively and continuously with no intervals between successive scans and were completed within 15 minutes after injection of the contrast agent. Acquisition times for the various sequences were as follows: axial 2D-T1W SE: 2 minutes 20 seconds, 3D-T1W BB CUBE: 2 minutes 35 seconds, 3D-T1W fast SPGR: 2 minutes 26 seconds, and coronal 2D-T1W SE: 3 minutes 40 seconds. To avoid timing bias after contrast injection, we alternated the order of the two 3D sequences (3D-T1W BB CUBE and 3D-T1W fast SPGR) for

all 42 patients by rotation. There were no differences in the time-interval between gadolinium injection and the BB CUBE and SPGR scanning sequences.

Table 1 : Imaging parameters for the phantom and clinical studies

	T1W	T2W	FLAIR	T1W SE	T1W BB CUBE	T1W fast SPGR
FOV (cm)	22*22	22*22	22*22	22*22	22*22	22*22
Matrix size	320*320	288*320	256*192	320*320	224*224	224*224
TR (ms)	500	4000	8802	500	500	9.6
TE (ms)	13	82.1	127	13	17.8	4.20
FA	90	90	90	90	90	20
Slice thickness (mm)	6	6	6	6	2	2
NEX	1	1	1	1	1	1
Scan time (min:sec)	2:20	2:32	2:59	2:20	2:35	2:26
parallel imaging factor	-	-	-	-	2	1.25
echo train length	-	-	-	-	24	-

T1W SE, T1W BB CUBE, and T1W fast SPGR sequences were utilized in both the phantom and clinical studies.
T1W: T1-weighted
T2W: T2-weighted
FLAIR: fluid attenuated inversion recovery
SE: spin echo
BB: black blood
SPGR: spoiled gradient-echo sequence
FOV: field of view
TR: repetition time
TE: echo time
FA: flip angle
NEX: number of excitations

Image analysis

Post-contrast axial 3D-T1W BB CUBE and 3D-T1W fast SPGR pulse sequences were compared with regard to the lesion detectability and the CR [(CR) = (SI of lesion – SI of normal white matter (WM)) / SI of normal WM].

A general radiologist (H.H., 18 years of experience as a radiologist) and a neuroradiologist (R.A., 31 years of experience as a radiologist) evaluated images with regard to the lesion detectability in a blinded fashion. If there was a discrepancy between the radiologists, consensus was reached through subsequent discussion.

To assess the detectability of the lesions, each lesion was counted, measured, and classified in accordance

with its largest measured dimension in any imaging plane as either ≥ 5 mm or < 5 mm. The existence of contrast-enhanced lesions was determined in all images（including conventional, T1W BB CUBE, and T1W fast SPGR images）. Differences between the number of enhanced lesions detected by each reader using each sequence and the criterion for the standard number of enhanced lesions were calculated. Additionally, each reader evaluated the images after a 3-month interval to allow us to measure differences between the number of enhanced lesions, calculate the criterion for the standard number of enhanced lesions detected using each sequence, and determine the intra-observer agreement. To eliminate bias, the T1W BB CUBE images were analyzed initially at the first reading whereas the T1W fast SPGR images were analyzed initially at the second reading performed 1 week after the first. Multiplanar 3D reconstructed images and other images were also assessed if needed.

Because surgical confirmation was not available for some of the subjects, the existence of the lesions was classified as true positive if the size or number of enhanced lesions increased on follow-up MR images（either BB CUBE or SPGR）and/or CT scans. MR and/or CT data were obtained for all patients with enhanced brain lesions. Lumbar puncture and cerebrospinal fluid examination were performed only in two cases when carcinomatous meningitis was suspected on the basis of clinical symptoms and MRI findings.

In all images, the region of interest（ROI）was set at 5.6 mm² and placed at the area with the highest intensity in the lesion. The CR was measured for all lesions larger than 5.6 mm² that could be identified on 3D-T1W BB CUBE and 3D-T1W fast SPGR images, while lesions smaller than 5.6 mm², ring-enhanced thin-walled lesions, lesions in the vicinity of the brain surface, and lesions associated with inflammatory/infectious diseases were excluded. Tumor necrosis was not included in the ROI. We set the cut-off point as 5.6 mm² because it was the smallest ROI that could be set manually on our DICOM viewer. Each lesion was measured and classified as either larger or smaller than 5 mm according to its largest dimension in the axial plane based on 3D-T1W BB CUBE images. Then the CR of each lesion was calculated and compared between the different sequences.

Statistical Analysis

The differences in the detectability of neoplastic lesions between T1W BB CUBE, T1W fast SPGR, and T1W SE images were evaluated using a test of difference in ratios（two-sample test for proportions）. Inter-observer and intra-observer agreement for lesion detectability was tested using the kappa coefficient（κ）. Interpretation of the coefficient followed the method proposed by Ladis and Kock[6], i.e., κ < 0: no agreement, 0–0.20: slight, 0.21–0.40: fair, 0.41–0.60: moderate, 0.61–0.80: substantial, and 0.81–1: almost perfect agreement. The CR of each lesion was calculated and compared between the 3D-T1W BB CUBE and 3D-T1W fast SPGR sequences using paired t-tests. Statistical analyses were performed using R software（version 3.2.4, R Core Team, Vienna, Austria）and p<0.05 was considered statistically significant.

Results

Phantom study

CRs of the phantom tubes relative to normal white matter are shown in Fig. 1 for 2D-T1W SE, 3D-T1W BB CUBE, and 3D-T1W fast SPGR sequences. CR increased linearly as the gadolinium concentration increased for all of the sequences in the range of 0.125-1.25 mmol/L. With this working concentration, CR values from 2D-T1W SE, 3D-T1W BB CUBE, and 3D-T1W fast SPGR sequences appeared to be equivalent. At gadolinium concentrations above 1.25 mmol/L, CR values from 3D-T1W BB CUBE and 3D-T1W fast SPGR images started to decrease, whereas CR values from 2D-T1W SE images continued to increase until the gadolinium concentration reached 2.5 mmol/L.
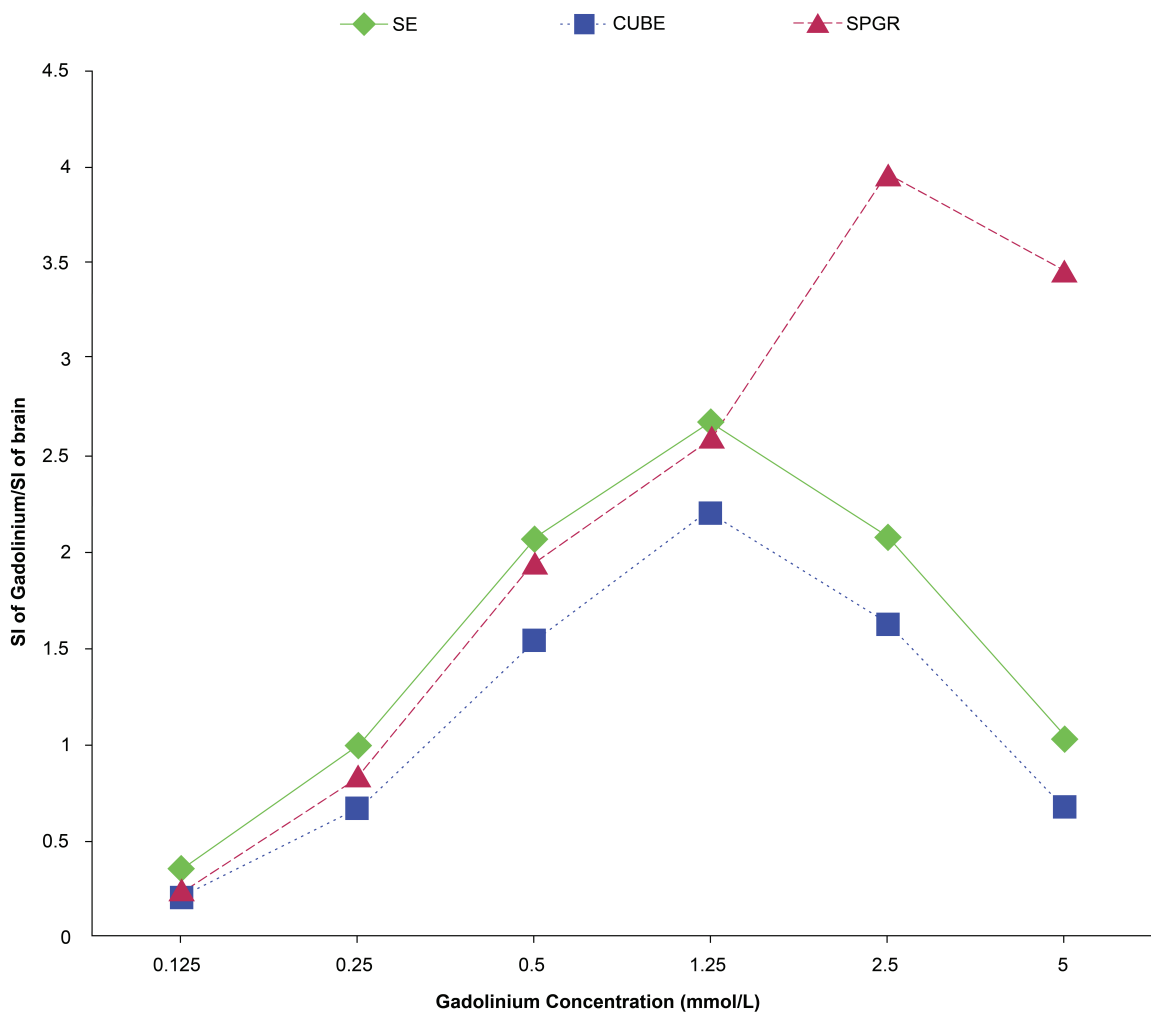
Figure 1 : CR values for 2D-T1W SE, 3D-T1W BB CUBE, and 3D-T1W fast SPGR images acquired with an FA of 20 degrees in the phantom study. The vertical axis shows CR: CR = (SI of sample tube – SI of white matter) / SI of white matter. CR increased as the Gd-DTPA concentration increased for all of the sequences. At all gadolinium concentrations, the highest CR was seen on 2D-T1W SE images, followed by 3D-T1W fast SPGR images. At a Gd-DTPA concentration of 0.125 mmol/L, the CR on 3D-T1W BB CUBE images was almost equivalent to that on 3D-T1W fast SPGR images. [Abbreviations - CR: contrast ratio, SE: spin echo, BB: black blood, SPGR: Spoiled gradient-echo, SI: signal intensity]

Clinical study

Abnormal enhanced lesions were observed in 25 of the 42 subjects, specifically, brain metastases in 17 subjects; glioma, 3 subjects; meningioma, 2 subjects; oligodendroglioma, 1 subject; malignant lymphoma, 1 subject; malignant glioma, 1 subject. In 6 subjects with metastases, 3 subjects with glioma, 1 subject with oligodendroglioma, 1 subject with malignant glioma, and 1 subject with malignant lymphoma, the diagnosis was confirmed through biopsy. False positive tumor detection did not occur in the study cohort. The diagnosis of each lesion and the basis for making the diagnosis are summarized in Table 2.

Table 2 : Diagnoses of the lesions and basis

Patient number	Number of lesions	Age/sex	Diagnosis	Basis for diagnosis
1	4	69/F	Metastasis（Lung cancer）	Increase in size or number
2	0	55/M	Astrocytoma	Operative findings
3	16	62/F	Metastasis（Lung cancer）	Operative findings
4	0	60/F	Metastasis（Breast cancer）	Increase in size or number
5	1	67/F	Meningioma	Confirmed by follow-up MRI
6	1	50/M	Diffuse astrocytoma	Operative findings
7	9	76/F	Metastasis（Lung cancer）	Increase in size or number
8	0	74/M	Metastasis（Prostate cancer）	Increase in size or number
9	2	60/M	Metastasis（Lung cancer）	Increase in size or number
10	11	68/F	Metastasis（Lung cancer）	Increase in size or number
11	3	65/M	Glioblastoma	Operative findings
12	2	65/M	Oligoastrocytoma	Operative findings
13	1	65/F	Malignant lymphoma	Biopsy
14	15	69/F	Metastasis（Lung cancer）	Biopsy
15	1	33/M	Glioblastoma	Operative findings
16	0	35/M	Metastasis（Lung cancer）	Increase in size or number
17	10	68/M	Metastasis（Lung cancer）	Operative findings
18	12	52/F	Metastasis（Breast cancer）	Operative findings
19	0	40/F	Carcinomatous meningitis（Lung cancer）	Cerebrospinal fluid examination
20	1	65/F	Metastasis（Lung cancer）	Operative findings
21	1	65/M	Malignant melanoma	Increase in size or number
22	9	68/F	Metastasis, Carcinomatous meningitis（Lung cancer）	Increase in size or number, Cerebrospinal fluid examination
23	1	48/M	Metastasis（Lung cancer）	Increase in size or number
24	7	32/F	Metastasis（Lung cancer）	Increase in size or number
25	13	54/F	Metastasis（Lung cancer）	Increase in size or number

This study was performed from April to August 2013.

The detectability of enhanced lesions and its relationship with lesion size in Gd-2D-T1WI (SE), T1W BB CUBE, and T1W fast SPGR images are summarized in Table 3. In the 25 subjects with enhanced lesions, a total of 120 lesions were detected through MR examination. All of the lesions (55/55 lesions ≥ 5 mm in diameter and 65/65 lesions < 5 mm in diameter) were observed on 3D-T1W BB CUBE images. In comparison, 111/120 lesions (54/55 of ≥ 5 mm lesions and 57/65 of < 5 mm lesions) were detected on 3D-T1W fast SPGR images, and only 90/120 lesions (53/55 of ≥ 5 mm lesions and 37/65 of < 5 mm lesions) were identified in Gd-2D-T1W SE scans. The detectability of enhanced lesions was significantly better in 3D-T1W BB CUBE than 3D-T1W fast SPGR sequences for lesions < 5 mm (p=0.011), but was no different for lesions ≥ 5 mm (p=1.00, Table 3). Assessment of the inter-observer and intra-observer agreement of lesion detectability revealed moderate agreement between 3D-T1W BB CUBE and 3D-T1W fast SPGR sequences. The inter-observer κ coefficients were 0.69 and 0.67 for 3D-T1W BB CUBE and 3D-T1W fast SPGR sequences, respectively, while the intra-observer κ coefficients were 0.78 and 0.76, respectively.

Table 3 : Contingency table showing relationship between the size and detectability of lesions in T1W BB CUBE and T1W fast SPGR sequences (n=120 lesions in 25 patients, 54 lesions ≥ 5 mm in diameter and 57 lesions < 5 mm in diameter)

	T1W SE	T1W BB CUBE	T1W fast SPGR	P-value (T1W BB CUBE vs T1W fast SPGR)
Lesions ≥ 5 mm	53/55 (96%)	55/55 (100%)	54/55 (98%)	1.000
Lesions < 5 mm	37/65 (57%)	65/65 (100%)	57/65 (88%)	0.011

T1W BB CUBE: T1-weighted black blood CUBE
T1W fast SPGR: T1-weighted fast spoiled gradient-echo sequence

Of the 9/120 lesions that were not detected on 3D-T1W fast SPGR images, 1 lesion was ≥ 5 mm in diameter (Fig. 2) and 8 were < 5 mm in diameter. In the subject shown in Fig. 3, although the lesion was found on 3D-T1W BB CUBE images, it was difficult to identify on 3D-fast SPGR images because it was close to the tentorial sinus. In the subject shown in Fig. 4, a lesion less than 5 mm in diameter was found on 3D-T1W BB CUBE images, but was difficult to visualize on 3D-T1W fast SPGR images. Carcinomatous meningitis was detected in 2 subjects, but was difficult to identify on 3D-T1W fast SPGR images in one of them (Fig. 5).
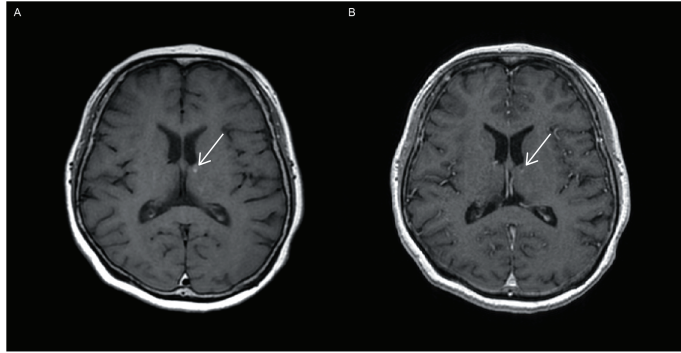
Figure 2 : (a) Contrast-enhanced 3D-T1W BB CUBE image and (b) contrast-enhanced 3D-T1W fast
SPGR image from a 54-year-old patient with multiple metastases of primary lung cancer
(patient # 25, Table 2). Although a lesion ≥ 5 mm in diameter is seen on the 3D-T1W BB
CUBE image, the lesion is difficult to identify on the 3D-T1W fast SPGR image (arrow).
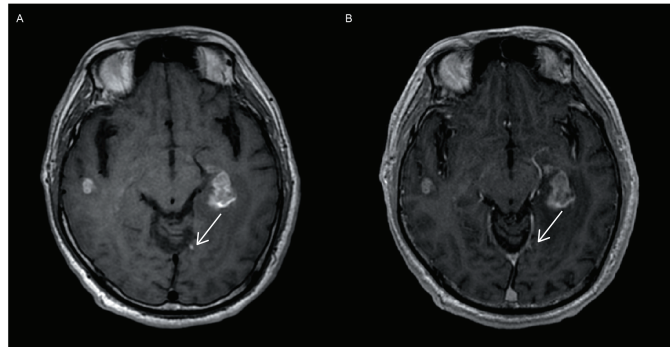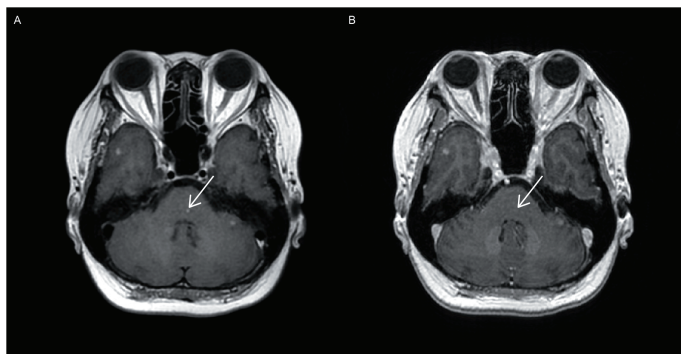[Abbreviations - BB: black blood, SPGR: Spoiled gradient-echo]

Figure 3 : (a) Contrast-enhanced 3D-T1W BB CUBE image and (b) contrast-enhanced 3D-T1W fast
SPGR image from a 52-year-old patient with multiple metastases of primary breast cancer
(patient # 18, Table 2). Although a lesion is seen on the 3D-T1W BB CUBE image, it is diffi-
cult to identify on the 3D-T1W fast SPGR image because it is near the tentorial sinus (arrow).
[Abbreviations - BB: black blood, SPGR: Spoiled gradient-echo]

Figure 4 : (a) Contrast-enhanced 3D-T1W BB CUBE image and (b) contrast-enhanced 3D-T1W fast
SPGR image from a 54-year-old patient with multiple metastases of primary lung cancer
(patient # 25, Table 2). A contrast-enhanced lesion can be identified in the pons on the
3D-T1W BB CUBE image, but not on the 3D-T1W fast SPGR image (arrow). [Abbreviations
- BB: black blood, SPGR: Spoiled gradient-echo]

Figure 5：（a）Contrast-enhanced 3D-T1W BB CUBE image and （b）contrast-enhanced 3D-T1W fast SPGR image from a 40-year-old patient with multiple metastases of primary lung cancer and carcinomatous meningitis （patient ＃ 19, Table 2）. Supratentorial carcinomatous meningitis （indicated by a circle）is identified on the 3D-T1W BB CUBE image, but not the 3D-T1W fast SPGR image. ［Abbreviations - BB: black blood, SPGR: Spoiled gradient-echo］

The CR was measured for 111/120 lesions （54 lesions ≥ 5 mm in diameter and 57 lesions < 5 mm in diameter）that were observed on both 3D-T1W BB CUBE and 3D-T1W fast SPGR images for the 25 subjects （Fig. 6）. The CRs of 3D-T1W BB CUBE and 3D-T1W fast SPGR sequences for lesions ≥ 5 mm （0.66±0.36 vs. 0.56±0.30, p=0.153）were not significantly different, but were significantly lower in 3D-T1W BB CUBE images compared to 3D-T1W fast SPGR images for lesions < 5 mm（0.29±0.19 vs. 0.39±0.21, p=0.006）（Table 4）.
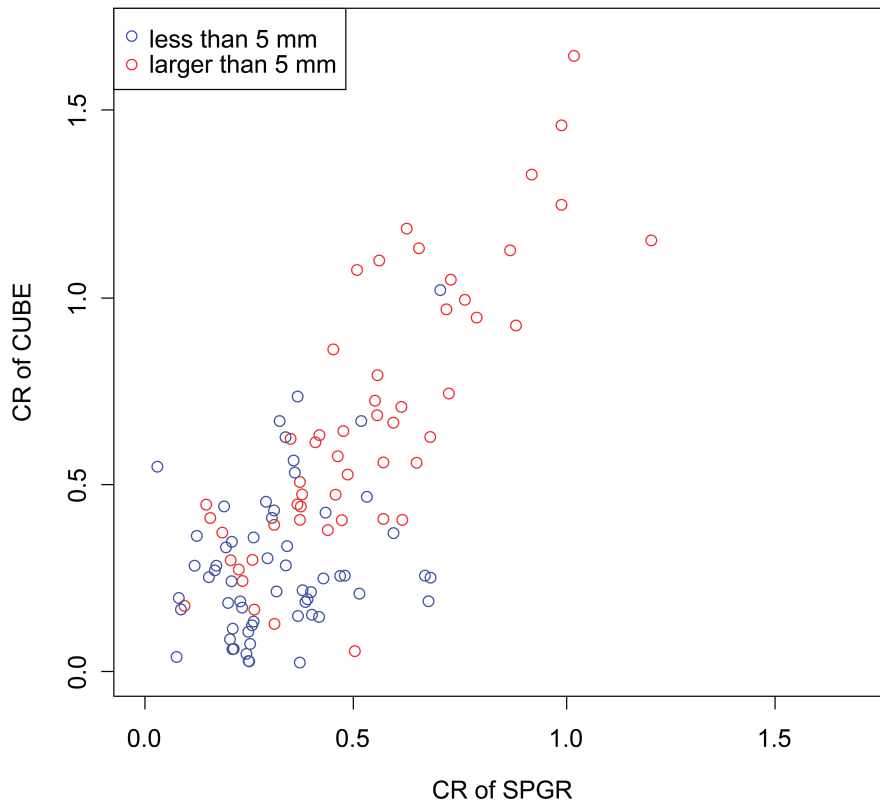

Figure 6：Scatter diagram of CR values of 3D-T1W BB CUBE and 3D-T1W fast SPGR images. The blue markers indicate lesions < 5 mm and red markers indicate lesions ≥ 5 mm.

Table 4 : Contrast Ratio （CR; mean ±standard deviation） of entire study cohort for lesions ≥ 5 mm and < 5 mm under different imaging sequences.

	T1W SE	T1W BB CUBE	T1W fast SPGR	P-value （T1W BB CUBE vs T1W fast SPGR）
Lesions ≥ 5 mm	0.56±0.36	0.66±0.36	0.56±0.30	0.153
Lesions < 5 mm	0.23±0.18	0.29±0.19	0.39±0.21	0.006

T1W SE: T1-weighted spin echo

T1W BB CUBE: T1-weighted black blood CUBE

T1W fast SPGR: T1-weighted fast spoiled gradient-echo sequence

Discussion

This study showed that the detectability of intracranial lesions was higher with BB CUBE than SPGR images, and the difference in detectability was greater for lesions < 5 mm in diameter. Among 8 lesions < 5 mm in diameter that were undetectable with SPGR, we could not identify 7 lesions at all and the remaining lesion was difficult to see because it was near the tentorial sinus. These results highlight the superiority of post-contrast 3D-T1W BB CUBE images over 3D-T1W fast SPGR sequences in improving the detectability of small lesions < 5 mm in diameter during 1.5-T MRI.

Our results also suggest that a diameter of < 5 mm is critical for lesion detection. Lesions larger than 5 mm in diameter were readily detected on images obtained with almost all sequences, including 3D-T1W BB CUBE and 3D-T1W fast SPGR. Only 1 lesion ≥ 5 mm in diameter that was found on 3D-T1W BB CUBE images proved difficult to identify on 3D-T1W fast SPGR images, and this lesion showed very thin ring-like enhancement. Our results are in agreement with previous studies that have shown improved detection of smaller lesions （< 10 mm in diameter） compared to larger lesions after contrast enhancement [7].

Our phantom study showed a linear increase in the signal intensity of normal white matter with different concentrations of the contrast agent. However, CR on BB CUBE and SPGR sequences were similar at the working gadolinium concentration of 0.125-1.25 mmol/L. In contrast, in the clinical study, we observed differences in CR between the two sequences. It was interesting that several lesions < 5 mm in diameter that were undetectable by SPGR could be identified by BB CUBE, although the mean CR was higher with SPGR than with BB CUBE images. This suggests that factors other than CR also likely contribute to lesion detectability. Since white matter/gray matter contrast has been reported to be better on SPGR than SE images, strong T1 contrast may have resulted in lesions having a lower signal intensity than the surrounding normal brain tissue on SPGR images before contrast enhancement and this signal gap could cancel the effect of contrast enhancement [8, 9]. For example, if lesions exhibit a low intensity signal, CR is also likely to be low on post-contrast images. Indeed, SungWoon et al. [2] have reported lower contrast enhancement on CUBE

FLAIR images compared to BB CUBE and T1W-SE images owing to superior T1 contrast in CUBE FLAIR images without contrast-enhancement.

Another factor related to the high detectability of lesions on BB CUBE images could be the magnetization transfer（MT）effect observed with fast SE techniques such as BB CUBE and SPACE [7, 10]. Fast SE techniques require multiple refocus pulses, which are off-resonance, provide a greater MT effect, and reduce the background signal in BB CUBE compared to SPGR sequences [11]. For these reasons, post-contrast 3D-T1W BB CUBE images were excellent for detecting small lesions < 5 mm in diameter and for finding carcinomatous meningitis. In addition, SPGR sequences did not show flow-related artifacts, but the high luminal signal sometimes made it difficult to distinguish lesions in the cortex or on the dura mater, as has been reported in other studies [3, 10]. Using SPACE, 3D FSE with variable FA refocusing, it was reported that a low FA refocusing pulse results in a strong flow void effect but the luminal signal remained [3]. Application of flow dephasing for 3D-T1W BB CUBE images allows full suppression of vessel signals, which is very useful for the detection of small lesions, especially in the posterior cranial fossa and on the brain surface [2].

There were some limitations in this study. First, the two sequences were started at different times after injection of the contrast agent. However, it has been reported that the CNR of enhanced lesions vs. gray matter shows no significant differences between 3.5 minutes and 25 minutes after contrast injection [12, 13]. Second, we could not obtain histological confirmation of the diagnosis for some subjects. Although some false-positive lesions may have been included in our study, we believe that careful observation and interpretation of previous and/or follow-up imaging data minimized the possibility of false positives. Third, we measured CR as a parameter in this study because calculation of the signal-to-noise ratio and CNR cannot be performed accurately with only one set of images when parallel imaging is performed, and the subtraction method is preferred for evaluating these parameters on scans obtained with parallel imaging [14]. Last, the lesions used for CR measurement were relatively large and tended to show good gadolinium uptake, while the lesions that showed differential detectability among the sequences were small and weakly enhanced. Although we measured the CR of lesions smaller than those reported in the literature, it is a limitation that our data did not include CR values for a larger number of small（< 5.6 cm²）and poorly enhanced lesions（superficial brain/ dural lesions）.

Conclusion

When 1.5-T MRI is performed, post-contrast 3D-T1W BB CUBE images seem to be superior to 3D-T1W fast SPGR sequences and provide better detectability of small lesions < 5 mm in diameter.

References

1．Park J, Kim EY. Contrast-enhanced, three-dimensional, whole-brain, black-blood imaging：application to small brain metastases. Magn Reson Med. 2010;63:553–61.

2．SungWoon I, Ashikaga R, Yagyu Y, Wakayama T, Miyoshi M, Hyodo T, et al. Contrast enhancement of intracranial lesions at 1.5T：comparison among 2D spin echo, black-blood（BB）Cube, and BB Cube-FLAIR sequences. Eur Radiol. 2015;25:3175–86.

3．Komada T, Naganawa S, Ogawa H, Matsushima M, Kubota S, Kawai H, et al. Contrast-enhanced MR imaging of metastatic brain tumor at 3 tesla：utility of T1-weighted SPACE compared with 2D spin echo and 3D gradient echo sequence. Magn Reson Med Sci. 2008;7:13–21.

4．Reichert M, Morelli JN, Runge VM, Tao A, von Ritschl R, von Ritschl A, et al. Contrast-enhanced 3-dimensional SPACE versus MP-RAGE for the detection of brain metastases：considerations with a 32-channel head coil. Invest Radiol. 2013;48:55–60.

5．Kato Y, Higano S, Tamura H, Mugikura S, Umetsu A, Murata T, et al. Usefulness of contrast-enhanced T1-weighted sampling perfection with application-optimized contrasts by using different flip angle evolutions in detection of small brain metastasis at 3T MR imaging：comparison with magnetization-prepared rapid acquisition of gradient echo imaging. Am J Neuroradiol. 2009;30:923–9.

6．Landis JR, Koch GG. The measurement of observer agreement for categorical data. Biometrics. 1977;33:159–74.

7．Yuh WTC, Tali ET, Nguyen HD, Simonson TM, Mayr NA, Fisher DJ. The effect of contrast dose, imaging time, and lesion size in the MR detection of intracerebral metastasis. Am J Neuroradiol. 1995;16:373–80.

8．Brant-Zawadzki M, Gillan GD, Nitz WR. MP RAGE：a three-dimensional, T1-weighted, gradient-echo sequence initial experience in the brain. Radiology. 1992;182:769–75.

9．Chappell PM, Pelc NJ, Foo TK, Glover GH, Haros SP, Enzmann D. Comparison of lesion enhancement on spin-echo and gradient-echo images. Am J Neuroradiol. 1994;15:37–44.

10. Majigsuren M, Takashi AB, Kageji T, Matsuzaki K, Takeuchi M, Iwamoto S, et al. Comparison of Brain Tumor Contrast-enhancement on T1-CUBE and 3D-SPGR Images. Magn Reson Med Sci. 2016;15:34–40.

11. Constable RT, Anderson AW, Zhong J, Gore JC. Factors influencing contrast in fast spin-echo MR imaging. Magn Reson Imaging. 1992;10:497–511.

12. Melhem ER, Bert RJ, Walker RE. Usefulness of optimized gadolinium-enhanced fast fluid-attenuated inversion recovery MR imaging in revealing lesions of the brain. Am J Roentgenol. 1998;171:803–7.

13. Kakeda S, Korogi Y, Hiai Y, Ohnari N, Moriya J, Kamada K, et al. Detection of brain metastasis at 3T：comparison among SE, IR-FSE and 3D-GRE sequences. Eur Radiol. 2007;17:2345–51.

14. Goerner FL, Clarke GD. Measuring signal-to-noise ratio in parallel imaging MRI. Med Phys. 2011;38:5049–57.